Autofocusing imaging: Imaging with primaries, internal multiples and free-surface multiples

S. Singh[1], R. Snieder[1], J. Behura[1,3], J. van Der Neut[2], K. Wapenaar[2], E. Slob[2]
(1) Center for Wave Phenomena, Department of Geophysics, Colorado School of Mines, Golden, Colorado, USA
(2) Department of Geoscience and Engineering, Delft University of Technology, GA Delft, The Netherlands
(3) Seismic Science LLC, Colorado, USA

SUMMARY

Recent work on autofocusing with the Marchenko equation has shown how the Green's function for a virtual source in the subsurface can be obtained from reflection data. The response to the virtual source is the Green's function from the location of the virtual source to the surface. The Green's function is retrieved using only the reflection response of the medium and an estimate of the first arrival at the surface from the virtual source. Current techniques, however, only include primaries and internal multiples. Therefore, all surface-related multiples must be removed from the reflection response prior to Green's function retrieval. Here, we extend the Marchenko equation to retrieve the Green's function that includes primaries, internal multiples, and free-surface multiples. In other words, we retrieve the Green's function in the presence of a free surface. We use the associated Green's function for imaging the subsurface. The information needed for the retrieval are the reflection response at the surface and an estimate of the first arrival at the surface from the virtual source. The reflection response, in this case, includes the free-surface multiples; this makes it possible to include these multiples in the imaging operator and it obviates the need for surface-related multiple elimination.

INTRODUCTION

To focus a wavefield at a point in a medium only requires surface reflection data and an estimate of the first arriving wave at the surface from a point source at the focusing location (Broggini et al., 2012; Broggini and Snieder, 2012; Wapenaar et al., 2013). Unlike in seismic interferometry (Bakulin and Calvert, 2006), no receivers are required at the desired focusing location, i.e. the virtual source location. Significantly, the detailed medium parameters need not be known to focus the wavefield. However the travel-time of the direct-arrival of the virtual source to the surface is required. To obtain this travel time, one only needs a macro-model of the velocity.

The focusing scheme of Broggini et al. (2012), Broggini and Snieder (2012), and Wapenaar et al. (2013) is an extension of the algorithm of Rose (2002a,b) who shows an iterative scheme that solves the Marchenko equation for wavefield focusing in one dimension. The focused events in the wavefield for the virtual source consist of primaries and internal multiples (Wapenaar et al., 2013) but not free-surface multiples. Importantly, Rose (2002a,b) derived the focusing method (autofocusing) for single-sided illumination with sources and receivers on one side of the medium, similar to current geophysical acquisition methods.

The algorithm of Broggini et al. (2012) requires the removal of free-surface multiples from the reflection response of the medium to retrieve the Green's function by autofocusing. The removal of the free-surface multiples can be achieved by Surface Related Multiple Elimination (SRME) (Verschuur et al. (1992)).

Wapenaar et al. (2011a) illustrate imaging with the Green's function in 1D and also discuss how to image in multi-dimensions (2D and 3D). Similarly, Behura et al. (2012) introduce an imaging algorithm based on the auto-focusing scheme that images not only primaries but also internal multiples, thereby reducing imaging artifacts. Broggini et al. (2014) extend the work of Behura et al. (2012) by using multidimensional deconvolution (MDD) as the imaging condition in place of conventional cross-correlation or deconvolution, which further reduces the artifacts. In other words, Broggini et al. (2014) retrieve the Green's function from the acquisition surface to any point in the medium. This Green's function is essentially an imaging or downward continuation operator. Since this Green's function includes both primaries and internal multiples, we expect improved subsurface images compared to using primaries alone.

In this paper, we modify the earlier focusing algorithms (Rose, 2002a; Broggini et al., 2012; Wapenaar et al., 2013) to focus not only primaries and internal multiples but also the free-surface multiples. We achieve such focusing using reflected waves in the presence of a free surface and an estimate of the first arrival from the focus location to the surface. Notably, our proposed auto-focusing scheme obviates the need for SRME.

The free surface is the strongest reflector in the system; therefore, in general, the free-surface multiples are stronger than internal multiples. In addition, free-surface multiples can be used to provide better illumination, higher fold, and better vertical resolution of the subsurface (Schuster et al., 2003; Jiang et al., 2007; Muijs et al., 2007a,b). For these reasons, by retrieving the Green's function which includes primaries and all multiples (including free-surface multiples) and using the imaging condition proposed by Behura et al. (2012), we expect better imaging of the subsurface.

THEORY

The theory of focusing the wavefield without a free surface, i.e. retrieving the Green's function G_0, is discussed by Rose (2002a), Broggini et al. (2012), and Wapenaar et al. (2013). In our notation, any wavefield quantity with a subscript 0 (e.g R_0) signifies that no free-surface multiples are present. In the focusing scheme of Broggini et al. (2012), and Wapenaar et al. (2013) they remove the free-surface multiples from the reflection response R (by SRME) to get R_0 and then compute G_0, the Green's function in the absence of the free surface.

We generalize the formulation of Wapenaar et al. (2013) to include free-surface multiples. In our case, the reflections from the free surface are included in the focusing scheme similar to the treatment by Wapenaar et al. (2004) of free-surface multiples; hence no SRME is required.

We begin by defining our spatial vector field by its horizontal coordinates and depth coordinates, for instance, $\mathbf{x_0} = (\mathbf{x_H}, x_{3,0})$, where $\mathbf{x_H}$ are the horizontal coordinates at a depth $x_{3,0}$. We define a solution for the waves that focus at a point in a medium, called the focusing solutions. Wapenaar et al. (2013) define two focusing solutions; f_1 and f_2. The f_1 solution involves waves that focus at $\mathbf{x}'_\mathbf{i}$ at a defined depth level (∂D_i) for incoming and outgoing waves at the acquisition surface (∂D_0) at $\mathbf{x_0}$. The solution f_2 is somewhat the opposite of f_1 as it is a solution for waves that focus just above ∂D_0 at $\mathbf{x}''_\mathbf{0}$ for incoming and outgoing waves at ∂D_i. The focusing solutions exist in a reference medium that has the same material properties as the actual inhomogeneous medium between ∂D_0 and ∂D_i and that is homogeneous above ∂D_0 and reflection-free below ∂D_i. Therefore, the boundary conditions on ∂D_0 and ∂D_i in the reference medium, where the focusing solution exist, are reflection free. Note that this boundary condition need not be the same as the actual medium. The focusing solutions can be separated into up-going and down-going waves; the first focusing solution in the frequency domain reads (Wapenaar et al. (2013))

$$f_1(\mathbf{x}, \mathbf{x}'_\mathbf{i}, \omega) = f_1^+(\mathbf{x}, \mathbf{x}'_\mathbf{i}, \omega) + f_1^-(\mathbf{x}, \mathbf{x}'_\mathbf{i}, \omega), \tag{1}$$

while the second focusing solution reads

$$f_2(\mathbf{x}, \mathbf{x}''_\mathbf{0}, \omega) = f_2^+(\mathbf{x}, \mathbf{x}''_\mathbf{0}, \omega) + f_2^-(\mathbf{x}, \mathbf{x}''_\mathbf{0}, \omega). \tag{2}$$

In this paper the superscirpt $(+)$ refer to down-going waves and $(-)$ to up-going waves.

We find relationships between the focusing solutions by separating these solutions into one-way wavefields (Wapenaar et al., 2013) and applying these wavefields to reciprocity theorems, Wapenaar and Grimbergen (1996). For instance, in the frequency domain, the up-going wavefield of f_1 at ∂D_0 is $f_1^-(\mathbf{x_0}, \mathbf{x}'_\mathbf{i}, \omega)$ while the down-doing wavefield is $f_1^+(\mathbf{x_0}, \mathbf{x}'_\mathbf{i}, \omega)$. At or just below ∂D_i, the up-going wavefield of f_1 vanishes since in the reference medium below ∂D_i is homogeneous, while the down-going wavefield is $f_1^+(\mathbf{x_i}, \mathbf{x}'_\mathbf{i}, \omega) = \delta(\mathbf{x_H} - \mathbf{x}'_\mathbf{H})$. The solution f_2 is separated into one-way wavefields using similar reasoning, (more details of the relationships between these solutions are given in Wapenaar et al. (2013)). The relationship between the focusing solutions are (Wapenaar et al., 2013):

$$f_1^+(\mathbf{x}''_\mathbf{0}, \mathbf{x}'_\mathbf{i}, \omega) = f_2^-(\mathbf{x}'_\mathbf{i}, \mathbf{x}''_\mathbf{0}, \omega), \tag{3}$$

and

$$-f_1^-(\mathbf{x}''_\mathbf{0}, \mathbf{x}'_\mathbf{i}, \omega)^* = f_2^+(\mathbf{x}'_\mathbf{i}, \mathbf{x}''_\mathbf{0}, \omega). \tag{4}$$

The wavefields in our actual medium can also be separated into one-way wavefields at the different depth levels, i.e. ∂D_0 and ∂D_i, as shown in Figure 1. Note, that the additional one-way wavefields that are added to the actual medium, in our case, in the presence of the free surface in comparison to without the

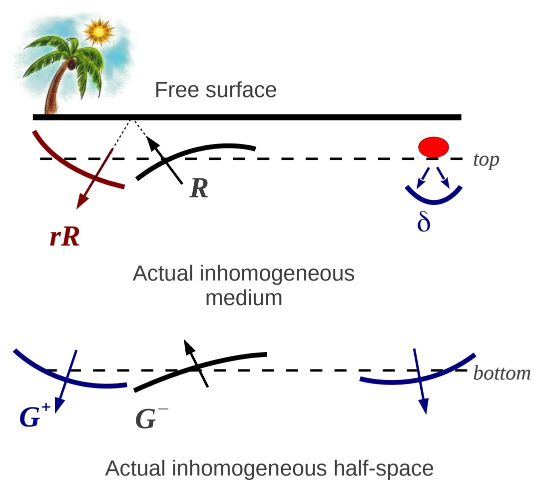

Figure 1: Green's functions in the actual inhomogeneous medium in the presence of a free surface.

free surface are the reflected waves from the free surface rR. In Figure 1, rR denotes the reflected waves from the free surface, where r is the reflection coefficient of the free surface and R are the recorded reflected waves from the subsurface. Consequently, in our case, the Green's functions at the different depth levels all include reflected waves from the free surface.

We use the convolution and cross-correlation reciprocity theorems to find relationships for the one-way wavefields of f_1 and the wavefields in the actual medium:

$$\begin{aligned} G^-(\mathbf{x}'_\mathbf{i}, \mathbf{x}''_\mathbf{0}, \omega) = & \int_{\partial D_0} [f_1^+(\mathbf{x_0}, \mathbf{x}'_\mathbf{i}, \omega) R(\mathbf{x_0}, \mathbf{x}''_\mathbf{0}, \omega) \\ & - r f_1^-(\mathbf{x_0}, \mathbf{x}'_\mathbf{i}, \omega) R(\mathbf{x_0}, \mathbf{x}''_\mathbf{0}, \omega)] d\mathbf{x} - f_1^-(\mathbf{x}''_\mathbf{0}, \mathbf{x}'_\mathbf{i}, \omega), \end{aligned} \tag{5}$$

and

$$\begin{aligned} G^+(\mathbf{x}'_\mathbf{i}, \mathbf{x}''_\mathbf{0}, \omega) = & -\int_{\partial D_0} [f_1^-(\mathbf{x_0}, \mathbf{x}'_\mathbf{i}, \omega)^* R(\mathbf{x_0}, \mathbf{x}''_\mathbf{0}, \omega) \\ & - r f_1^+(\mathbf{x_0}, \mathbf{x}'_\mathbf{i}, \omega)^* R(\mathbf{x_0}, \mathbf{x}''_\mathbf{0}, \omega)] d\mathbf{x} + f_1^+(\mathbf{x}''_\mathbf{0}, \mathbf{x}'_\mathbf{i}, \omega)^*. \end{aligned} \tag{6}$$

where * represents the complex conjugate, and $r = -1$ is the reflection coefficient of the free surface. R is flux normalized so that the one-way reciprocity equations (Wapenaar and Grimbergen (1996)) holds. Note the up-going Green's function (G^-) in the actual inhomogeneous medium at ∂D_0 is the reflection response R for a downward radiating source at ∂D_0.

The two-way Green's function is obtained by adding equations 5 and 6 as well as using equations 1, 2 and the relationship between f_1 and f_2 (equations 3 and 4):

$$\begin{aligned} & G(\mathbf{x}'_\mathbf{i}, \mathbf{x}''_\mathbf{0}, \omega) = f_2(\mathbf{x}'_\mathbf{i}, \mathbf{x}''_\mathbf{0}, \omega)^* + \\ & \int_{\partial D_0} [f_2(\mathbf{x}'_\mathbf{i}, \mathbf{x_0}, \omega) + r f_2(\mathbf{x}'_\mathbf{i}, \mathbf{x_0}, \omega)^*] R(\mathbf{x_0}, \mathbf{x}''_\mathbf{0}, \omega) d\mathbf{x_0}. \end{aligned} \tag{7}$$

We retrieve G the same way we retrieve G_0 as discussed in Wapenaar et al. (2013), except we use equation 7 instead of equation 8 for the Green's function equation.

$$G_0(\mathbf{x_i}', \mathbf{x_0}'', \omega) = f_2(\mathbf{x_i}', \mathbf{x_0}'', \omega)^* + \int_{\partial D_0} f_2(\mathbf{x_i}', \mathbf{x_0}, \omega) R_0(\mathbf{x_0}, \mathbf{x_0}'', \omega) d\mathbf{x_0}. \tag{8}$$

Equation 8 is the expression to retrieve the Green's function which includes primaries and internal multiples but not free-surface multiples. Importantly, equation 7 simplifies to equation 8 in the limiting case when $r \to 0$ since we will no longer have reflections from the free surface.

Similar to our treatment of the focusing function f_2, we can define another focusing function g_2 such that

$$g_2(\mathbf{x}, \mathbf{x_0}'', \omega) = f_2^+(\mathbf{x}, \mathbf{x_0}'', \omega) - f_2^-(\mathbf{x}, \mathbf{x_0}'', \omega). \tag{9}$$

Analogously, we can define a difference Green's function $\widetilde{G}$ that is related to g_2 similar to expression 7 by

$$\begin{aligned}\widetilde{G}(\mathbf{x_i}', \mathbf{x_0}'', \omega) &= g_2(\mathbf{x_i}', \mathbf{x_0}'', \omega)^* \\ &- \int_{\partial D_0} g_2(\mathbf{x_i}', \mathbf{x_0}, \omega) R(\mathbf{x_0}, \mathbf{x_0}'', \omega) d\mathbf{x_0} \\ &+ r \int_{\partial D_0} g_2(\mathbf{x_i}', \mathbf{x_0}, \omega)^* R(\mathbf{x_0}, \mathbf{x_0}'', \omega) d\mathbf{x_0}.\end{aligned} \tag{10}$$

We call $\widetilde{G}$ the difference Green's function since

$$\widetilde{G}(\mathbf{x_i}', \mathbf{x_0}'', \omega) = G^+(\mathbf{x_i}', \mathbf{x_0}'', \omega) - G^-(\mathbf{x_i}', \mathbf{x_0}'', \omega). \tag{11}$$

To yield the up-going Green's function, we subtract equations 7 and 11:

$$G^-(\mathbf{x_i}', \mathbf{x_0}'', \omega) = 1/2[G(\mathbf{x_i}', \mathbf{x_0}'', \omega) - \widetilde{G}(\mathbf{x_i}', \mathbf{x_0}'', \omega)]. \tag{12}$$

Similarly, we obtain the down-going Green's function by adding equations 7 and 11:

$$G^+(\mathbf{x_i}', \mathbf{x_0}'', \omega) = 1/2[G(\mathbf{x_i}', \mathbf{x_0}'', \omega) + \widetilde{G}(\mathbf{x_i}', \mathbf{x_0}'', \omega)]. \tag{13}$$

These up- and down-going (G^+ and G^-) Green's functions at the focal point are used for imaging and include primaries and all multiples. The up- and down-going Green's functions have been used for imaging the subsurface, (Behura et al., 2012; Broggini et al., 2014, 2012; Wapenaar et al., 2011a). However, their Green's function only contains primaries and internal multiples. In this paper, the up- and down-going Green's function also includes free-surface multiples.

The use of up- and down-going wavefield for imaging is not a new principle. Claerbout (1971), Wapenaar et al. (2000) and Amundsen (2001) have shown that one can get the reflection coefficient below an arbitrary depth level once the up- and down-going wavefields are available. The governing equation for imaging with these up- and down-going waves is

$$\begin{aligned}&G^-(\mathbf{x_i}', \mathbf{x_0}'', t) \\ &= \int_{\partial D_i} d\mathbf{x_i} \int_{-\infty}^{\infty} G^+(\mathbf{x_i}', \mathbf{x_0}'', t - t') R_0^{\cup}(\mathbf{x_i}, \mathbf{x_i}', t') dt',\end{aligned} \tag{14}$$

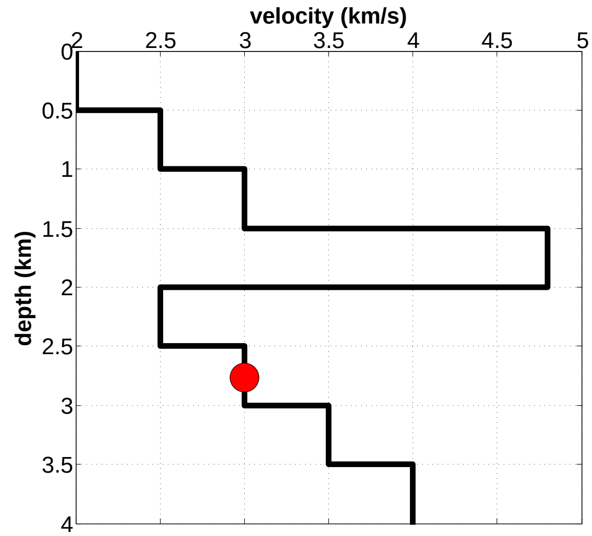

Figure 2: Velocity model with high impedance layer at 1.5 km; the dot is the position of the virtual source.

where ∂D_i is an arbitrary depth level, $R_0^{\cup}$ is the reflection response below ∂D_i. In addition, $R_0^{\cup}$ at ∂D_i is reflection-free above this depth level. We can think of $R_0^{\cup}$ as the reflection response from a truncated medium; where the truncated medium is the same as the true medium below ∂D_i and reflection free above. Equation 14 states that we can recover G^- from the convolution of G^+ with $R_0^{\cup}$ and integrate along all source positions x' of $R_0^{\cup}$.

We solve for $R_0^{\cup}$ by multidimensional deconvolution (Wapenaar et al., 2008, 2011b) as the time integral is a convolution. The subsurface image is given by taking the zero lag of $R_0^{\cup}$, i.e. $t = 0$ at each depth level in the model, (for each ∂D_i), this is called the multidimensional imaging condition. Alternatively, once we obtain $R_0^{\cup}$ at an arbitrary ∂D_i we can also apply a standard imaging procedure to image below ∂D_i. This is because $R_0^{\cup}$ is the reflection response of the truncated medium below ∂D_i for sources and receivers at ∂D_i.

NUMERICAL EXAMPLE

We consider a 1D model that has a high impedance layer generic to salt models as shown in Figure 2. A Receiver at the surface records the reflected waves. To retrieve the Green's function in 1D, one needs the travel time of the first arriving wave from the virtual source to the surface. In 2D or 3D media, a smooth version of the slowness (1/velocity) can be used to get an estimate of the direct arriving wave from the virtual source to the surface. The direct arriving wave can be obtained using finite-difference modeling of the waveforms.

We obtain the focusing function f_2 by setting the left-hand side of equation 7 to zero and evaluating this expression for a time earlier than the first arriving wave. The focusing function is substituted in equation 7 to retrieve the Green's function lo-

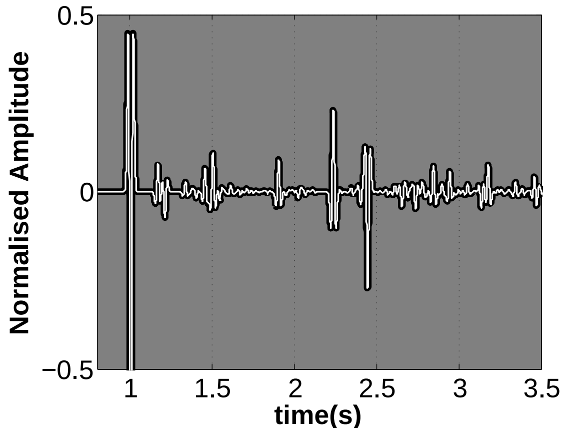

Figure 3: Retrieved Green's function (normalized by maximum amplitude), G, from a depth of 2.75 km to the surface (white). The model Green's function is displayed (in black) in the background.

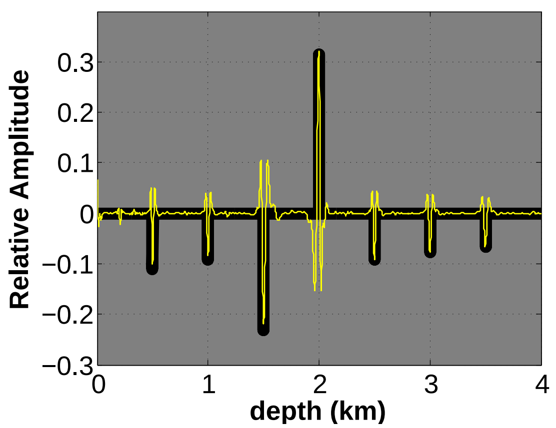

Figure 4: Autofocusing imaging of Figure 2 in yellow, with the true reflectivity (in black) in the background.

cated at 2.75 km to the surface, Figure 3. This Green's function G, arbitrarily scaled to its maximum amplitude (Figure 3), is the response at the surface ∂D_0 to the virtual source (located at 2.75 km [dot in Figure 2]).

We also model the Green's function using finite differences to ensure that the Green's function retrieved from our autofocusing algorithm is accurate, and superimposed this result on Figure 3. The vertical scale of Figure 3 is enlarged to better illustrate the model and retrieved Green's function. For this reason, the first arrival at time 1.0 s is clipped. The corresponding autofocus image of the model in Figure 2 illustrates the correct location of the reflectors as well as the correct scaled reflection coefficient shown in Figure 4. In 1D, the autofocus image is the deconvolution of the up- and down-going Green's function at each image point for $t = 0$. There are some anomalous amplitudes in the autofocus image (especially around 200 m) but they are small compared to the actual reflectors' amplitude.

DISCUSSION/CONCLUSION

In summary, we extended the retrieval of the Green's function to include the presence of a free surface. This function includes primaries, internal multiples, and now free-surface multiples. Significantly, our proposed method does not require any surface-related multiple removal of the reflection response. Although we show 1D numerical examples, the equations that solve for the Green's function are multidimensional as well as our imaging condition, thus our autofocusing imaging (which uses primaries, internal multiples and free surface multiples) is extendable in 2D and 3D. In addition, we need an estimate of the first arrival at the surface from the virtual source in the subsurface. To obtain the first arrival, we only need a macro model of the velocity, but the small scale details of the velocity and density need not be known.

ACKNOWLEDGMENTS

This work was funded by the sponsor companies of the Consortium Project on Seismic Inverse Methods for Complex Structures. We are grateful to Diane Witters for her help in preparing this manuscript.

REFERENCES

Amundsen, L., 2001, Elimination of free-surface related multiples without need of the source wavelet: Geophysics, **66**, 327–341.

Bakulin, A., and R. Calvert, 2006, The virtual source method: Theory and case study: Geophysics, **71**, SI139–SI150.

Behura, J., K. Wapenaar, and R. Snieder, 2012, Newton-Marchenko-Rose imaging, *in* SEG Technical Program Expanded Abstracts 2012: Society of Exploration Geophysicists, 1–6.

Broggini, F., and R. Snieder, 2012, Connection of scattering principles: a visual and mathematical tour: European Journal of Physics, **33**, 593–613.

Broggini, F., R. Snieder, and K. Wapenaar, 2012, Focusing the wavefield inside an unknown 1d medium: Beyond seismic interferometry: Geophysics, **77**, A25–A28.

Broggini, F., R. Snieder, K. Wapenaar, and J. Behura, 2014, Wave field autofocusing and imaging with multidimensional deconvolution: numerical examples for reflection data with internal multiples: submitted to Geophysics.

Claerbout, J., 1971, Toward a unified theory of reflector mapping: Geophysics, **36**, 467–481.

Jiang, Z., J. Sheng, J. Yu, G. Schuster, and B. Hornby, 2007, Migration methods for imaging different-order multiples: Geophysical Prospecting, **55**, 1–19.

Muijs, R., A. Robertsson, J. O., and K. Holliger, 2007a, Prestack depth migration of primary and surface-related multiple reflections: Part I: Imaging: Geophysics, **72**, S59–S69.

———, 2007b, Prestack depth migration of primary and surface-related multiple reflections: Part II: Identification and removal of residual multiples: Geophysics, **72**, S71–S76.

Rose, J., 2002a, 'Single-sided'autofocusing of sound in layered materials: Inverse problems, **18**, 1923–1934.

———, 2002b, Time reversal, focusing and exact inverse scattering: Imaging of complex media with acoustic and seismic waves, 97–106.

Schuster, G. T., Z. Jiang, and J. Yu, 2003, Imaging the most bounce out of multiples: Presented at the 65th Annual Conference, EAGE Expanded Abstracts: session on Multiple Elimination.

Slob, E., K. Wapenaar, F. Broggini, and R. Snieder, 2014, Seismic reflector imaging using internal multiples with marchenko-type equations: Geophysics, **79**, S63–S76.

Verschuur, D., A. Berkhout, and C. Wapenaar, 1992, Adaptive surface-related multiple elimination: Geophysics, **57**, 1166–1177.

Wapenaar, C., and J. Grimbergen, 1996, Reciprocity theorems for one-way wavefields: Geophysical Journal International, **127**, 169–177.

Wapenaar, K., F. Broggini, E. Slob, and R. Snieder, 2013, Three-dimensional single-sided marchenko inverse scattering, data-driven focusing, green's function retrieval, and their mutual relations: Phys. Rev. Lett., **110**, no. 8, 084301.

Wapenaar, K., F. Broggini, R. Snieder, et al., 2011a, A proposal for model-independent 3D wave field reconstruction from reflection data: 2011 SEG Annual Meeting, Society of Exploration Geophysicists, 3788–3792.

Wapenaar, K., J. Fokkema, M. Dillen, P. Scherpenhuijsen, et al., 2000, One-way acoustic reciprocity and its applications in multiple elimination and time-lapse seismics: Presented at the 2000 SEG Annual Meeting, Society of Exploration Geophysicists.

Wapenaar, K., E. Slob, and R. Snieder, 2008, Seismic and electromagnetic controlled-source interferometry in dissipative media: Geophysical Prospecting, **56**, 419–434.

Wapenaar, K., J. Thorbecke, and D. Draganov, 2004, Relations between reflection and transmission responses of three-dimensional inhomogeneous media: Geophysical Journal International, **156**, 179–194.

Wapenaar, K., J. Van Der Neut, E. Ruigrok, D. Draganov, J. Hunziker, E. Slob, J. Thorbecke, and R. Snieder, 2011b, Seismic interferometry by crosscorrelation and by multidimensional deconvolution: a systematic comparison: Geophysical Journal International, **185**, 1335–1364.

Weglein, A., and W. Dragoset, 2007, Multiple attenuation: Society of Exploration Geophysicists, **23**, 482.